SiC MOSFETs for Offshore Wind Applications

IOP Conf. Series: Journal of Physics: Conf. Series **1104** (2018) 012032 doi:10.1088/1742-6596/1104/1/012032

SiC MOSFETs for Offshore Wind Applications

S Tiwari, T Undeland, O M Midtgård and R Nilsen

Norwegian University of Science and Technology, Department of Electric Power Engineering, NO-7491, Trondheim, Norway

E-mail: subhadra.tiwari@ntnu.no

Abstract. Space and weight are critical factors for offshore wind applications during the construction, operation, and maintenance phases. Superior material properties of silicon carbide enable the development of power devices capable of switching fast as well as handling high power. Thus, this paper performs the quantitative evaluation of the total converter loss and efficiency at different switching frequencies in order to observe the potential performance gains that SiC MOSFETs can bring over Si IGBTs for such applications. When simulating the detailed converter losses in a three-phase, two-level topology; the turn-on and turn-off switching energy losses obtained from the laboratory measurement and the conduction losses acquired from the datasheet are used as a look-up table input. Additionally, the simulated results are compared with the analytical and the numerical solutions. In conclusion, this analysis gives an insight into how SiC MOSFET outperforms Si IGBT over all switching frequency ranges with the advantages becoming more visible at higher frequencies.

1. Introduction

The potential power produced from wind is directly proportional to the cube of wind speed [1]. Compared to land, water has less surface roughness, so average wind speed is higher over open water, and consequently higher power potential. Moreover, offshore wind is stronger and steadier, whereas, onshore wind is disrupted by hills and buildings making it more turbulent. Besides, offshore wind turbines have less environmental constraints compared to those on onshore. These are some of the major driving forces for harvesting offshore wind energy [2].

For a long time silicon (Si)-based power devices have dominated the power electronics and power system applications. However, these devices are confronting some fundamental limits in the performance, such as breakdown voltage, operating temperature, and frequency, due to their inherent limitations of material properties. Recent literature in silicon carbide (SiC) has demonstrated the significant potential of SiC devices to fulfil such demands and requirements. Table 1 shows a comparison of the material properties of 4H-SiC with Si [3]. The column "factor", in Table 1, indicates the ratio of 4H-SiC versus Si where most of the material properties of SiC are superior than that of Si. For example, bandgap energy is about 3 times higher in SiC compared to Si which can be translated to switching devices with higher operating temperature; breakdown field intensity is about 10 times higher in SiC and this can lead to devices with higher breakdown voltage and still have the same conduction loss; higher thermal conductivity means faster heat dissipation which results in higher power density; and likewise, higher drift velocity enables faster transportation of carriers, and thereby faster switching of devices can be achieved. In offshore wind applications, space and weight savings are of paramount importance as these factors directly influence the cost and size of the mechanical design of the tower/nacelle.

The outstanding material properties of SiC can fulfil the demand because the power electronic conversion system with these devices will be compact, efficient, and thermally stable, and accordingly can be easily mounted in the nacelle of wind turbine.

Table 1. A comparison of material properties of 4H SiC with Si [3].

Material properties	Si	4H-SiC	Factor
Bandgap energy [eV]	1.12	3.26	2.9
Breakdown electric field [MV/cm]	0.23	2.2	9.56
Thermal conductivity [W/(cm.K)]	1.5	3.8	2.53
Electron mobility [$cm^2/(V.s) \times 10^3$]	1.4	0.95	0.67
Drift velocity [$cm/s \times 10^7$]	1	2.7	2.7
Dielectric constant	11.8	9.7	0.82

At present, most installed offshore wind turbines are based on relatively low voltage, < 690 V [4, 13]. On the other hand, the share of wind power is likely to increase in future as per the forecast [5], therefore a shift towards higher voltage is necessary to increase the power density of the system. For instance, for the same power, higher voltage means smaller current which leads to reduction in size of cable and power loss. In addition, high voltage SiC devices lead to simpler converter topologies resulting in high power density of the system.

SiC is recognised as a potential technology for wind power applications in [6, 7]. Reference [8] compared the performance of SiC MOSFET with Si IGBT, where the IGBT was non-punch through (NPT) type, optimised for the conduction loss. Similarly, in [9], a performance comparison between SiC MOSFET with punch through (PT) type of Si IGBT (optimised for the switching loss) was investigated. Note that an IGBT is a bipolar component; hence, carrier life time can be optimised as per the applications, i.e., a trade-off between switching loss (dv/dt) and conduction loss can be made. However, this paper covers the detail loss comparison at varying load current as an extension to the work presented in [9]. Most importantly, the loss in a back-to-back converter for offshore wind application is simulated using the experimentally measured data as a look-up table input in Section 4. Further, it verifies the simulation results with the numerical and analytical calculations. Finally, Section 5 summarises the major conclusions.

2. Methodology and measurement setup

A standard double pulse test methodology is used for evaluating the stresses, such as dv/dt, di/dt, and switching energy loss in the device under test (DUT). An equivalent circuit with a hard switched arrangement is shown in Fig. 1 a), where the current path during the turn-on and turn-off processes are routed by blue and green dotted lines. A low inductance hardware setup is displayed in Fig. 1 b). Switching current (I_d) is measured by a shunt resistor, SSDN - 414 - 01 (400 MHz, 10 $m\Omega$) from T&M research. In the similar manner, switching voltage (V_{ds}) is measured by high voltage differential probe (THDPO200, 200 MHz). The chosen measuring equipments prove to be good enough to track the transient waveforms of the selected devices [10]. An isolated gate driver with an adjustable output voltage is used for driving the SiC MOSFET where the gate voltage is set to 20 V for turn-on and -5 V for turn-off. The same gate driver is used for driving the Si IGBT with a small modification to achieve the required gate voltage ($\pm$ 15 V). Table 2 shows the key electrical parameters of the SiC MOSFET versus the Si IGBT taken at 25 °C and 125 °C from the manufacturers datasheet [11, 12]. R_{ds}/R_{ce} is the on-state resistance of MOSFET/IGBT, V_{CEO} is the on-state knee voltage, and R_d is the resistance of the free-wheeling diode. The column "difference" enlists the percentage increase (lead by + sign) or decrease (preceded by - sign) of the corresponding on-state parameters from 25 °C to 125 °C.

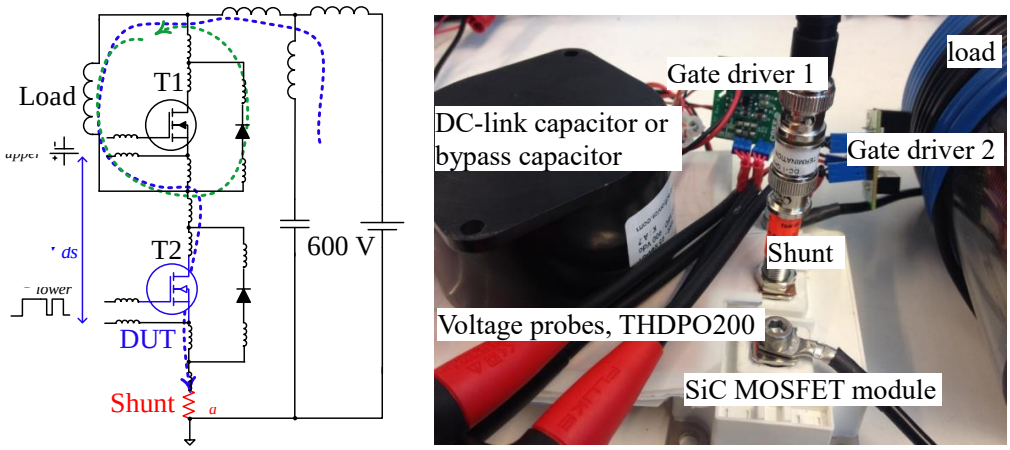

(a) Circuit diagram for double pulse test. (b) Hardware setup.

Figure 1. a) Circuit diagram illustrating the turn-on and turn-off processes in a buck converter during inductive clamped test. Upper transistor (T1) is always turned off by applying -5 V in the gate source (G_{upper}) while double pulses are given in the gate source (G_{lower}) of lower transistor (T2) which is also the DUT. b) Hardware setup showing a low inductance connection. An inductor with a single layer winding is used as load in order to ensure minimum stray capacitance (measured to be 10 pF using impedance analyser, E4990) so that the true switching characteristics of DUT are reflected.

Table 2. Key electrical parameters of SiC MOSFET versus Si IGBT module [11, 12].

Parameters	SiC MOSFET (Wolfspeed)			Si IGBT (Semikron)		
	25 (°C)	125 (°C)	difference (%)	25 (°C)	125 (°C)	difference (%)
R_{ds} / R_{ce} ($m\Omega$)	5.0	7.8	+36	6.3	7.6	+17
V_{CEO} (V)	Absent	Absent	Absent	1.4	1.7	+17
R_d ($m\Omega$), diode	2.25	4.35	+48	2.7	3.0	+10
V_{FO} (V), diode	0.925	0.83	−11	1.4	1.1	−27

Table 3. A summary of measurements of DUTs. V_{ds} = 600 V, I_d = 300 A and T_j = 25 °C.

Device Under Test	R_{goff} (Ω)	R_{gon} (Ω)	dv/dt (V/ns)	di/dt (A/ns)	E_{off} (mJ)	E_{on} (mJ)	E_{rec} (mJ)
SiC MOSFET	3.4	5	10.38	5.35	7.7	8.56	0.22
Si IGBT	0	2.35	16.64	5.7	7.67	24.9	13.6

3. Laboratory testing of SiC MOSFET versus Si IGBT module

Table 3 summarises a sample measurement of SiC MOSFET versus Si IGBT at V_{ds}/V_{ce} of 600 V, I_d/I_c of 300 A and T_j of 25 °C. Fig. 2 a) - d) exemplify the turn-on and turn-off transients of SiC MOSFET and Si IGBT for the summarised cases. For the selected value of gate resistances, the turn-off (E_{off}), turn-on (E_{on}) and total losses (E_{tot}) are plotted with varying load current, and are illustrated in Fig. 2 e) and f), which will be used as a look-up table input for the simulation of converter losses in Section 4.

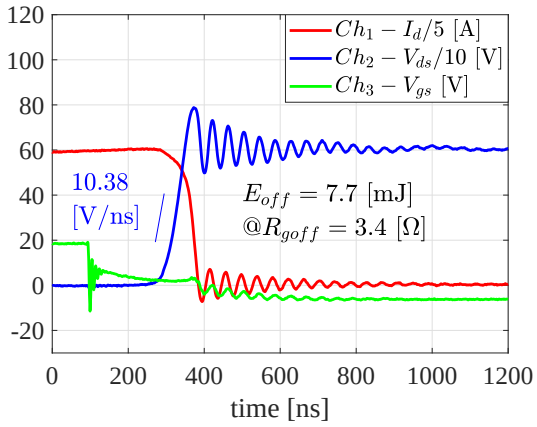

(a) Turn-off transient of SiC MOSFET I_d of 300 A.

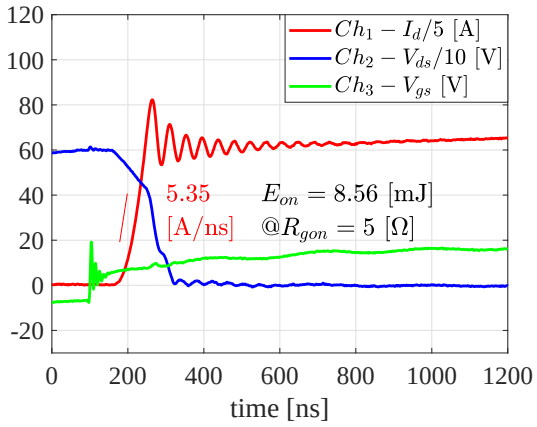

(b) Turn-on transient of SiC MOSFET I_d of 300 A.

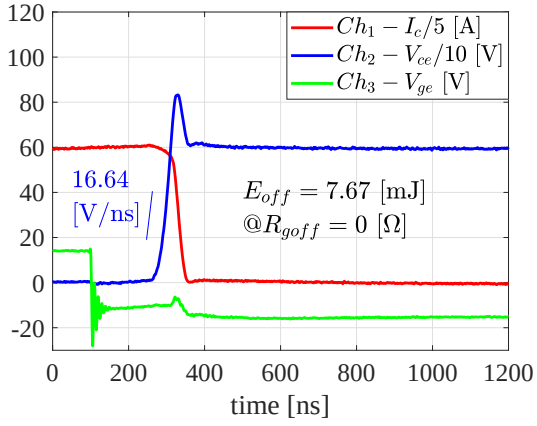

(c) Turn-off transient of Si IGBT I_c of 300 A.

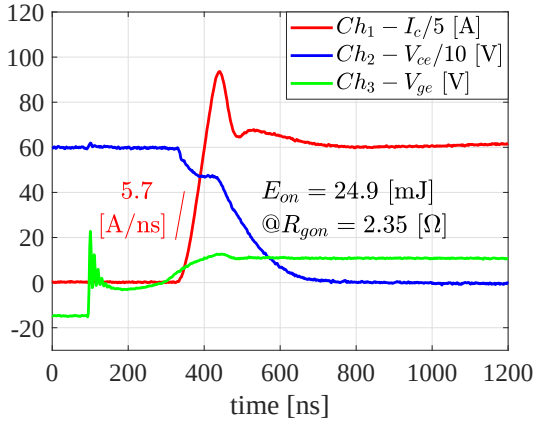

(d) Turn-on transient of Si IGBT I_c of 300 A.

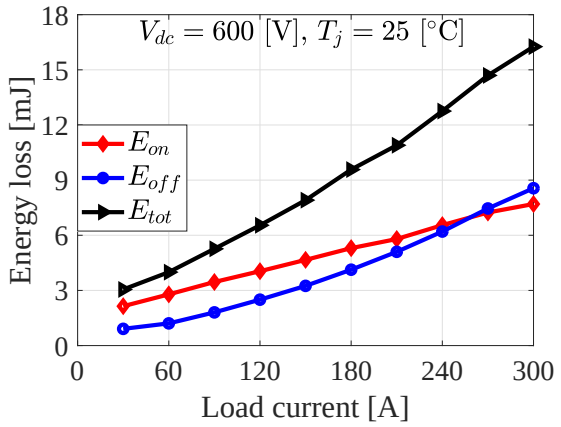

(e) Switching energy loss of SiC MOSFET V_{dc} of 600 V.

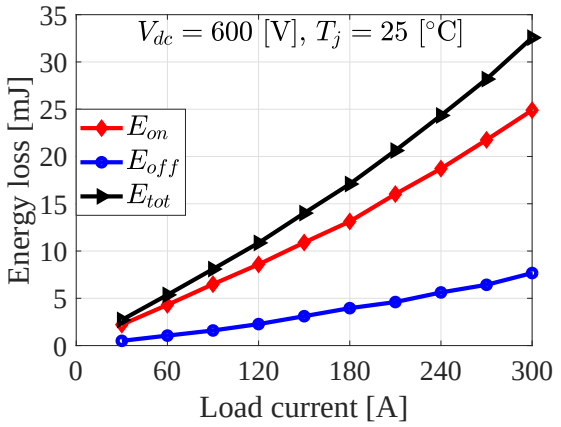

(f) Switching energy loss of Si IGBT V_{dc} of 600 V.

Figure 2. A sample of turn-off and turn-on transients of SiC MOSFET (a and b), Si IGBT (c and d) and plot of E_{on}, E_{off}, and E_{tot} of SiC MOSFET (e) and Si IGBT (f). Details about dv/dt during turn-off, di/dt during turn-on, E_{on}, and E_{off} for the chosen value of gate resistances (R_{gon}, R_{goff}) are labelled in the corresponding figures.

4. Selection of the converter topology and simulation of losses

The most popular and commercialised voltage source converter (VSC) topologies in offshore wind applications are mainly two: the first is three-phase, two-level type and the second is three-phase, three-level neutral point diode clamped (NPC) type [4, 13]. Former topology is employed for the low voltage and latter for the high voltage applications. These converters are mounted in a back-to-back configuration such that each share the same dc-link as illustrated in Fig. 3. One converter acts as a rectifier (connected on the generator-side) and another converter acts as an inverter (connected on the grid-side). When IGBTs/MOSFETs along with anti-parallel diodes are used, the converter allows bidirectional flow of power.

In this paper, the three-phase, two-level topology, as shown in Fig. 3, is chosen where the main purpose is to study the power losses in the back-to-back converter and perform the comparison between all-Si and all-SiC devices. Using MATLAB simulink, the switching loss obtained from the laboratory measurements and the conduction loss from the datasheet are used as a look-up table or polynomial functions based on the curve fitting for simulating the total converter loss. The loss is simulated for a space vector PWM (SVPWM) [14], dc-link voltage (V_{dc}) of 760 V, modulation index (m) of 1, and a load current (I_{orms}) of 300 A. The converter output voltage (V_{orms}) is about 460 V ($\sqrt{3}/(2 \cdot \sqrt{2}) \cdot V_{dc} \cdot$ m) and the power rating is approximately 240 kW.

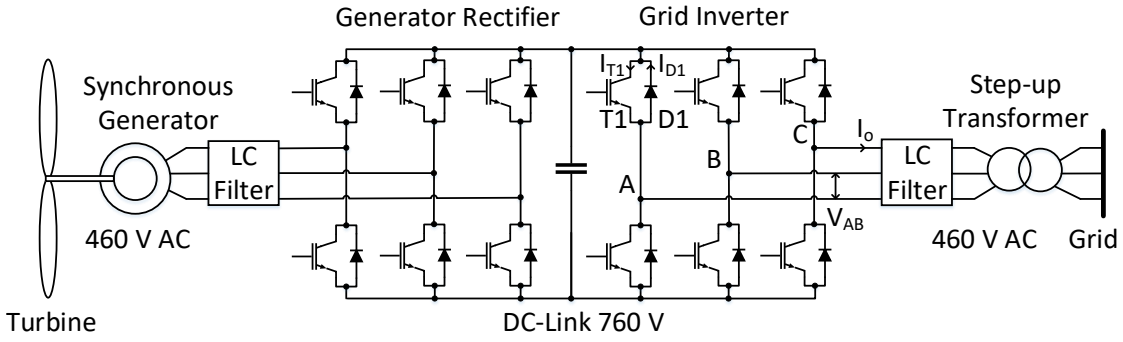

Figure 3. Schematic diagram of a three-phase, two-level back-to-back converter configuration for low voltage offshore wind applications. Current in one of the top switches and diodes of grid-side inverter is denoted by I_{T1} and I_{D1}, correspondingly.

4.1. Simulation results

Fig. 4 elucidates the simulated waveforms of the inverter-side such as output current (I_o), voltage between terminals A and B (V_{AB}), switching signal to IGBT T1, switching current in diode D1 (I_{D1}), switching current in IGBT T1 (I_{T1}), instantaneous power loss of IGBT T1, and average power loss of IGBT T1 with a filter of 0.01 (1/60) s. This sample plots are exemplified with switching frequency (f_{sw}) of 600 Hz, fundamental frequency of 60 Hz and m of 1.

4.2. Numerical verification of the simulation results

In the numerical verification method, the turn-on, turn-off, and total switching power losses of IGBT T1; $P_{sw-on-T1}$, $P_{sw-off-T1}$, and $P_{sw-tot-T1}$, correspondingly; are computed by counting the number of switching events during the fundamental cycle of the output. Table 4 lists the reading of currents and the corresponding energy losses from Fig. 5 a) and b), respectively. Note that Fig. 5 b) is derived from Fig. 2 f) by extrapolation of data from 300 A to 450 A using the same coefficients of polynomial as obtained by curve fitting the plot from 30 A to 300 A. The total sum of E_{on} is 133.3 mJ (11.8 + 34 + 50 + 31 + 6.49 = 133.3 mJ), and as a result $P_{sw-on-T1}$ of IGBT T1 is 10.13 W (133.3/1000 × 760/600 × 60 = 10.13 W). Similarly, the total

sum of E_{off} is 38.19 mJ and $P_{sw-off-T1}$ is 2.90 W, and thus, $P_{sw-tot-T1}$ is 13.03 W, as listed in Table 5 in the row named "Numerical". As the percentage differences between numerically calculated and simulated losses with reference to the numerical losses are below 4 %, as shown in Table 5,

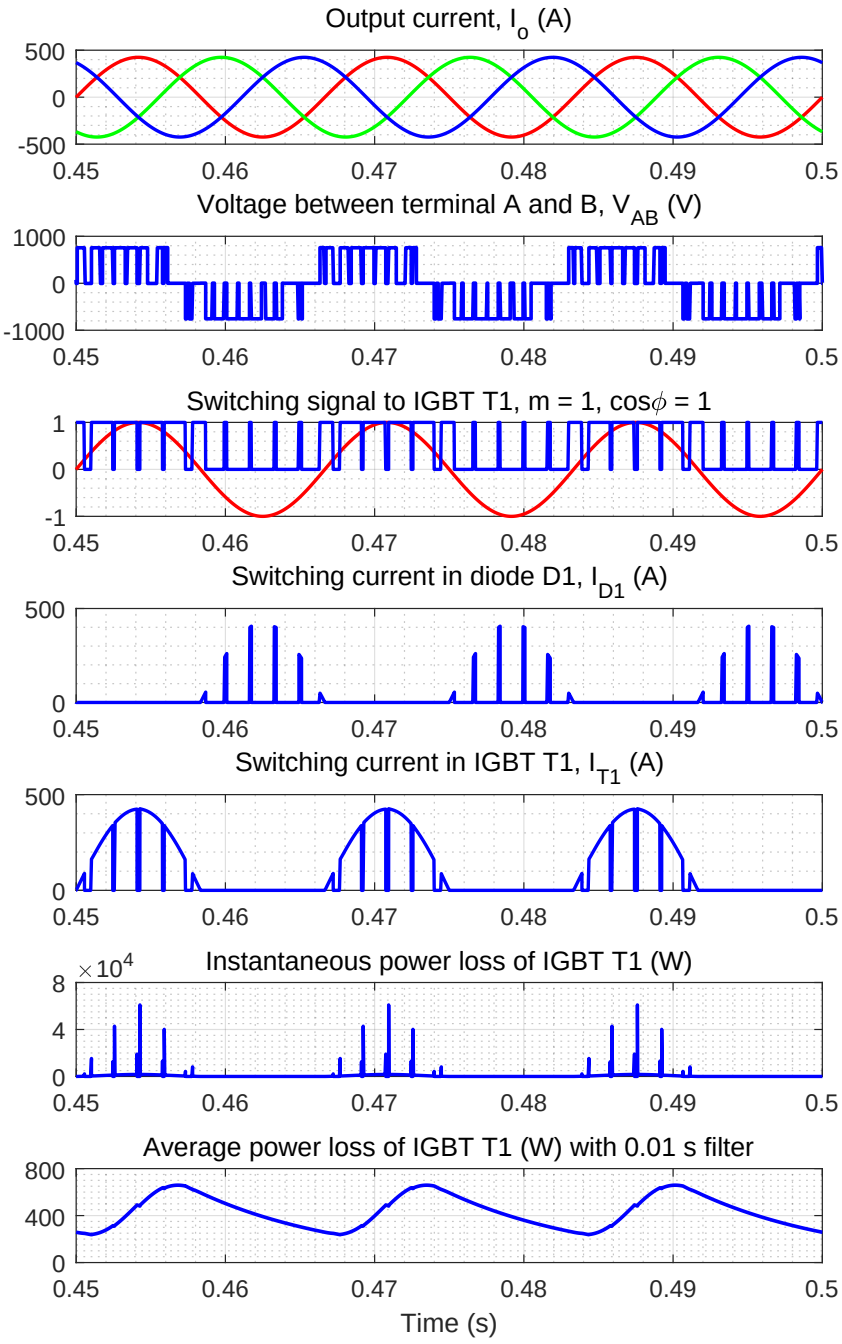

Figure 4. Illustration of the sample of simulated waveforms at various points in the schematic for the grid-side inverter in a standard two-level topology. With the dc-link voltage of 760 V, RMS output current of 300 A, $cos\phi$ of unity, modulation index of 1, and switching frequency of 600 Hz, the total simulated power loss of IGBT T1 is 433 W, the instantaneous and average power losses are displayed in lower 2 graphs.

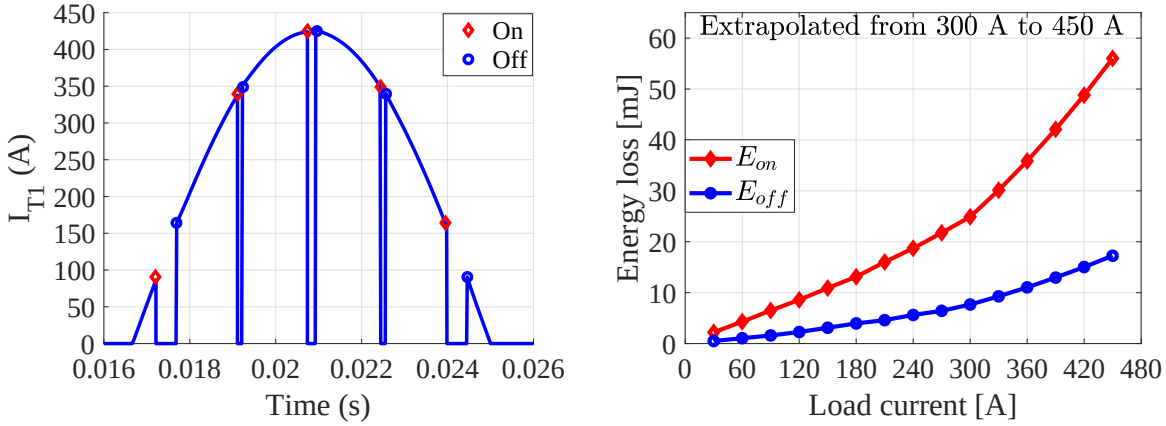

(a) Switching current in IGBT T1.

(b) Fig. 2 f) is extrapolated for current upto 450 A.

Figure 5. a) Detailed (zoomed in) view of switching current in IGBT T1. The RMS output current is 300 A, m is 1, $cos\phi$ is 1, fundamental frequency is 60 Hz, and switching frequency is 600 Hz. b) Extrapolation of Fig. 2 f) to fill in values in Table 4.

Table 4. Reading of currents and energy losses (refer Fig. 5 a and b).

I_{T1} [A]	90	160	340	350	425
E_{on}[mJ]	11.8	34	50	31	6.49
E_{off} [mJ]	1.59	10	12.8	10.4	3.4

Table 5. A comparison of simulated and numerically calculated power losses of transistor T1.

Power loss [W]	$P_{sw-on-T1}$	$P_{sw-off-T1}$	$P_{sw-tot-T1}$
Simulation	9.75	2.79	12.55
Numerical	10.13	2.90	13.03
Error [%]	3.75	3.79	3.68

4.3. Analytical verification of the simulation results

The switching loss of IGBT/MOSFET can be estimated using analytical approximations as long as the energy loss during switching is linearly dependent on the collector current, as given by Equation 1 [15]. Compared to the simulated results, as presented in Table 5, the error was found to be in the range of 5 % - 10 %. Moreover, considering the sinusoidal dependency of duty cycles versus time, the on-state power loss of IGBT ($P_{con-tr-T1}$) and diode ($P_{con-diode-D1}$) can be calculated by using Equation 2 and Equation 3, respectively [16, 17].

$$P_{sw-T1} = f_{sw} \cdot (E_{on} + E_{off}) \cdot \frac{\sqrt{2}}{\pi} \cdot \frac{I_{orms}}{I_{ref}} \cdot \frac{V_{dc}}{V_{ref}} \tag{1}$$

$$P_{con-tr-T1} = V_{CEO} \cdot I_o \cdot \left(\frac{1}{2 \cdot \pi} \pm \frac{m \cdot cos\phi}{8}\right) + R_{ce} \cdot I_o^2 \cdot \left(\frac{1}{8} \pm \frac{m \cdot cos\phi}{3 \cdot \pi}\right) \tag{2}$$

$$P_{con-diode-D1} = V_{FO} \cdot I_o \cdot \left(\frac{1}{2 \cdot \pi} \mp \frac{m \cdot cos\phi}{8}\right) + R_d \cdot I_o^2 \cdot \left(\frac{1}{8} \mp \frac{m \cdot cos\phi}{3 \cdot \pi}\right) \tag{3}$$

In these equations where ± are present, the upper sign applies for an inverter mode (motor operation) and lower sign for a rectifier mode (generator operation). For a MOSFET, the first term in Equation 2 will be zero because it does not possess knee voltage. For the better clarity, the description of symbols used in Equation 1 - 3 are enlisted in Table 6. The differences in analytically calculated and simulated conduction losses with respect to that with analytically calculated are found to be below 3 %.

Table 6. Definition of symbols used in Equation 1 - 3.

Symbol	Description	Value
V_{ref}	reference voltage	600 V
I_{ref}	reference current	300 A
ϕ	phase angle of current with respect to voltage	0° (inverter), 180° (rectifier)
I_o	peak output current	$\sqrt{2} \times I_{orms} = 424$ A
f_{sw}	switching frequency	1 kHz - 50 kHz
m	modulation index	1

4.4. Evaluation of inverter power loss at different switching frequencies
The detailed loss breakdown at various switching frequencies (1 kHz to 50 kHz) is shown in Fig. 6. The chosen IGBT is a PT type optimized for the fast switching over the conduction loss.

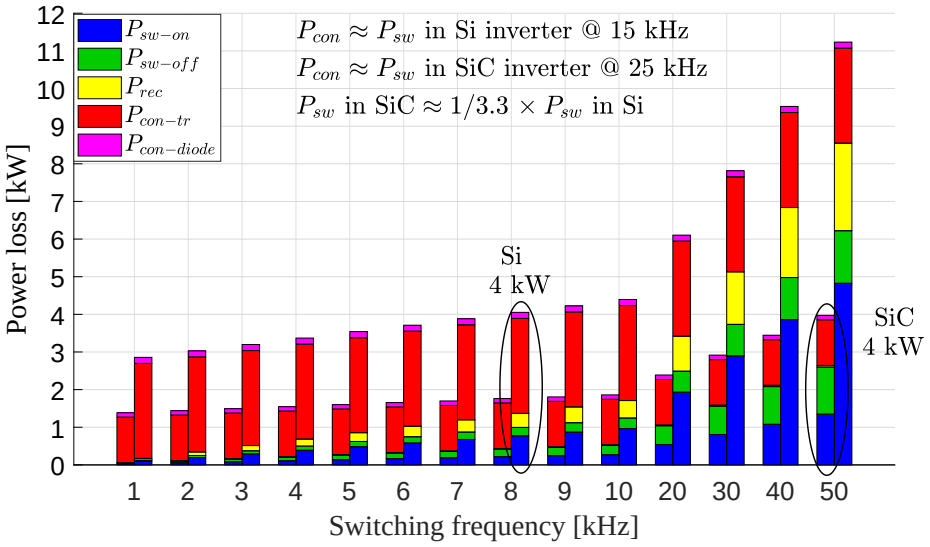

Figure 6. Breakdown of power loss in an inverter at different switching frequencies. The legends in bar chart are: turn-on switching loss (P_{sw-on}), turn-off switching loss (P_{sw-off}), diode recovery loss (P_{rec}), conduction loss in a transistor (P_{con-tr}), and conduction loss in a diode ($P_{con-diode}$). SiC MOSFET helps to reduce the switching loss, which is a dominant part of total loss in an IGBT inverter, particularly the P_{sw-on}. Inverter with SiC MOSFET can switch at higher frequency compared to that with Si IGBT with almost the same total power loss: an example of which is indicated in the bar chart where the frequency is about 6 times higher in SiC than in Si for the same total inverter power loss of about 4 kW.

Simulation results show that the conduction loss in the Si IGBT inverter is higher by a factor of 2 at 25 °C to that in the SiC MOSFET inverter. Furthermore, the results reveal that the total conduction loss (P_{con}) is approximately equal to the total switching loss (P_{sw}) at about 15 kHz and 25 kHz for the all-Si and all-SiC inverters, accordingly, i.e., for the low frequency region, the conduction loss is a dominating part of the total inverter loss. It should be pointed out that the turn-off power loss of the selected devices are almost equal because the PT IGBT switches off as fast as SiC MOSFET. The all-Si inverter has approximately 3.3 times higher P_{sw} than that with the all-SiC inverter, the major share being the combined loss of P_{sw-on} and P_{rec}. Therefore, in order to use Si IGBT at higher switching frequency, a practical solution would be the use of SiC diode as an anti-parallel diode instead of Si diode (a Hybrid solution) as this solution leads to the reduction in P_{rec}, and subsequently its influence on P_{sw-on}. Nonetheless, SiC MOSFET is a better solution over PT IGBT for all range of switching frequencies, unlike in a NPT IGBT, as discussed in the previous work, where the losses were comparable for lower frequencies ($\leq$ 3 kHz) [8].

4.5. Evaluation of back-to-back converter efficiency at different switching frequencies

A comparison of the total converter efficiency in a back-to-back converter using the all-SiC devices with the all-Si devices is depicted in Fig. 7. Converter with the SiC MOSFET shows 0.86 % and 5.04 % higher efficiencies at 1 kHz and 50 kHz, correspondingly over their Si IGBT counterparts, as marked in Fig. 7. The simulated switching losses of the back-to-back converters are equal, but the conduction losses are not. For instance, in the case of a rectifier mode, the simulated P_{con-tr} is lower and $P_{con-diode}$ is higher by a factor of 10 compared to those, correspondingly, in the case of an inverter mode.

Hence, SiC MOSFET offers lower on-state and switching losses compared to Si IGBT. Moreover, MOSFET structure possesses an intrinsic diode which switching performance is almost like a SiC Schottky diode, and thereby, the need of an additional anti-parallel diode can be eliminated, however, there is no such possibility in IGBT structure. The VSC with high voltage SiC MOSFETs (when available in $\approx$ 10 kV range) will be the most attractive candidate for high voltage direct current connections to offshore wind-farms as efficiency become more important.

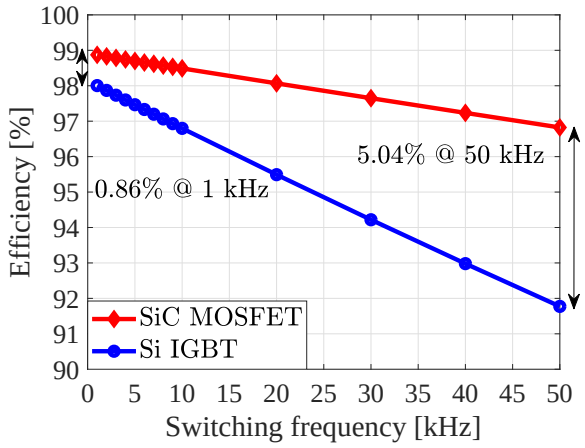

Figure 7. Comparison of a SiC MOSFET and a Si IGBT efficiencies in a three-phase back-to-back converter illustrates that at all the switching frequencies, the higher efficiency SiC MOSFET provide a performance advantage over their Si IGBT counterparts. At switching frequencies of 1 kHz, 3 kHz (practical at today's offshore applications) and 50 kHz, converter with the SiC MOSFET shows 0.86 %, 1.05 % and 5.04 % higher efficiencies over Si IGBT.

5. Conclusion

In conclusion, the simulation revealed that the solution with SiC MOSFET results in lower losses compared to that with Si IGBT over all the switching frequency ranges; the advantages of SiC being more pronounced at higher frequencies. For instance, the simulation showed that the back-to-back converter with SiC MOSFET is 0.86 % and 5.04 % more efficient at 1 kHz and 50 kHz, respectively over Si IGBT. Furthermore, it is also illustrated that for the same output power the inverter switching frequency can be increased by approximately 6 times in the SiC MOSFET compared to that in the Si IGBT with the similar total power loss. Besides, the conduction loss in Si based converter is 2 times and 1.56 times higher than those in SiC based at 25 °C and 125 °C, respectively. Thus, the reduction in loss can be utilized in a number of ways to optimize the circuit design, such as, increase efficiency, reduce cooling requirement. Especially, in a grid-connected offshore wind system, by increasing the operating frequency, the size of passive components, namely, filter and transformer, can be reduced resulting in higher power density of the system, which is a critical factor.

Acknowledgments

The authors would like to thank The Research Council of Norway and 6 industry partners who sponsor this project: EFD Induction, Siemens, Eltek, Statkraft, Norwegian Electric Systems, and Vacon.

References

[1] Elliott D L, Aspliden C I, Gowerl G L, Holladay C G and Schwartz M N 1987 Wind energy resource assessment of the Caribbean and Central America *Pacific Northwest National Laboratory (PNNL)*
[2] Kalmikov A 2017 Wind Power Fundamentals in *Wind Energy Engineering : A Handbook for Onshore and Offshore Wind Turbines* ed Letcher T M (Academic Press) chapter 2 17-24
[3] Östling M, Ghandi R and Zetterling C M 2011 SiC power devices - Present status, applications and future perspective in *IEEE 23rd Int. Symp. on Power Semiconductor Devices and ICs* San Diego CA 10-15
[4] Liserre M, Cardenas R, Molinas M and Rodriguez J 2011 Overview of Multi-MW Wind Turbines and Wind Parks in *IEEE Transactions on Industrial Electronics* **58** (4) 1081-1095
[5] Offshore wind, 2017, *GWEC*
Available: http://www.gwec.net/wp-content/uploads/2017/05/Global-Offshore-2016-and-Beyond.pdf
[6] Zhang H and Tolbert L M 2011 Efficiency Impact of Silicon Carbide Power Electronics for Modern Wind Turbine Full Scale Frequency Converter in *IEEE Transactions on Industrial Electronics* **58** (1) 21-28
[7] Lagier T, Ladoux P and Dworakowski P 2017 Potential of silicon carbide MOSFETs in the DC/DC converters for future HVDC offshore wind farms *in High Voltage*, **2** (4) 233-243.
[8] Tiwari S, Midtgård O M and Undeland T M 2016 SiC MOSFETs for future motor drive applications in *18th European Conf. on Power Electronics and Applications* Karlsruhe Germany 1-10
[9] Tiwari S, Midtgård O M and Undeland T M 2016 Comparative evaluation of a commercially available 1.2 kV SiC MOSFET module and a 1.2 kV Si IGBT module in *42nd Annual Conf. of the IEEE Industrial Electronics Society* Florence Italy 1093-1098
[10] Tiwari S, Langelid J K, Midtgård O M and Undeland T M 2017 Hard and soft switching losses of a SiC MOSFET module under realistic topology and loading conditions *19th European Conf. on Power Electronics and Applications* Warsaw Poland 1-10
[11] CAS300M12BM2 Datasheet 2014 *Cree Inc.*
[12] SKM400GB125D Datasheet 2007 *Semikron Inc.*
[13] Blaabjerg F and Ma K 2017 Wind Energy Systems in *Proceedings of the IEEE* **105** (11) 2116-2131
[14] Holmes D G and Lipo T A 2003 Zero Space Vector Placement Modulation Strategies in *Pulse Width Modulation for Power Converters:Principles and Practice* (Wiley-IEEE Press) chapter 6 259-336
[15] Wintrich A, Nicolai U, Tursky W and Reimann T 2015 *Application Manual Power Semiconductors SEMIKRON International GmbH*
[16] Graovac D and Pürschel M 2009 IGBT Power Losses Calculation Using the Data-Sheet Parameters *Application note Infineon Technologies AG*
[17] Lai J S, Young R W, Ott G W and McKeever J W 1995 Efficiency modeling and evaluation of a resonant snubber based soft-switching inverter for motor drive applications *26th Annual IEEE Power Electronics Specialists Conf.* Atlanta GA **2** 943-949